2021 60th IEEE Conference on Decision and Control (CDC)
December 13-15, 2021. Austin, Texas

Piecemeal Reduction of Models of Large Networks

Benjamin L. Francis[1], Mark K. Transtrum[1], Andrija T. Sarić[2] and Aleksandar M. Stanković[3]

2021 60th IEEE Conference on Decision and Control (CDC) | 978-1-6654-3659-5/21/$31.00 ©2021 IEEE | DOI: 10.1109/CDC45484.2021.9683471

***Abstract*— Many systems can be modeled as an intricate network of interacting components. Often the level of detail in the model exceeds the richness of the available data, makes the model difficult to learn, or makes it difficult to interpret. Such models can be improved by reducing their complexity. If a model of a network is very large, it may be desirable to split it into pieces and reduce them separately, recombining them after reduction. Such a distributed procedure would also have other advantages in terms of speed and data privacy. We discuss piecemeal reduction of a model in the context of the Manifold Boundary Approximation Method (MBAM), including its advantages over other reduction methods. MBAM changes the model reduction problem into one of selecting an appropriate element from a partially ordered set (poset) of reduced models. We argue that the prime factorization of this poset provides a natural decomposition of the network for piecemeal model reduction via MBAM. We demonstrate on an example network and show that MBAM finds a reduced model that introduces less bias than similar models with randomly selected reductions.**

I. Introduction

Complex systems often involve large, interconnected networks. Many times the complexity of the network makes it difficult to reason about the relevant mechanisms leading to the macro-scale behavior of the system. This complexity is typically reflected in the mathematical models used to predict and control these systems. In such cases, it is useful to have model reduction methods that preserve the interpretability of the model as a network of interconnected components.

Structure-preserving modifications of traditional model reduction methods, such as balanced truncation or Krylov subspace projection, have been explored in [1], [2], [3], [4], [5], [6]. Other approachs have included clustering ([7] and references therein) and static and dynamic equivalents ([8], [9], [10], [11], [12], [13], [14]).

Each of these methods has limitations. Some are only applicable to linear or linearized systems ([1], [3], [4], [5], [6], [7], [8], [12]). Others can only be used with first- or second-order components ([1], [7], [8], [9], [10]), or with components that are homogeneous ([7], [11]). For some methods it is not clear how to choose appropriate parameter values for the reduced subsystem models, so a separate parameter identification step is needed ([12], [13]). A few methods are intended for networks that have a specific sparsity structure ([8], [9], [10], [12]). Some can only be applied to whole systems, because reducing individual subsystems or components in open loop and then reconnecting them can make the system unstable [4]. Stability in physics-based models is often guaranteed by conservation laws, such as conservation of energy, mass, or charge, which provide natural Lyapunov functions for the system. Most existing structure-preserving reduction methods focus on the computational graph of a model but do not consider other desirable properties, such as internal conservation laws. In one recent approach [15], it has been shown that applying iterative Kron reduction and other reduction patterns to carefully selected graph structures in a power network preserves certain structural and physical properties of the system, such as graph sparsity and power-flow equivalence. But because each reduction pattern is paired with a specific type of graph structure, extending this approach to other types of structures is not straightforward.

Recent developments in information geometry have led to an alternative approach to model reduction known as the Manifold Boundary Approximation Method (MBAM) [16]. MBAM has previously been applied to models from systems biology and biophysics [16], [17], [18], [19], power systems [20], [21], [22], [23], [24], [25], and nuclear structure physics [26], and has been shown to be equivalent to balanced truncation and singular perturbation theory methods for linear time-invariant (LTI) systems in an appropriate parametrization [27]. Unlike other methods, MBAM maintains the physical interpretability of the model and can be used for arbitrary nonlinear systems. Rather than focusing on state variables (as do methods like balanced truncation), MBAM finds and applies parameter limits to the model which simplify its mathematical structure (which encodes both the topological structure of the network and the physics of the model's dynamics) without significantly impacting model accuracy. This means that all reductions correspond to physically-meaningful limiting behaviors of the model, and both the underlying conservation laws of the system and the physical interpretability of the model are maintained. In contrast to the approach in [15], MBAM reductions of network structure involve only two simple operations—cutting branches (edge removal) and merging nodes (edge contraction)—which can be applied anywhere in a network [24], [25]. Therefore, MBAM can be used to reduce networks with any topology. In addition, MBAM is a data-driven method, so reductions are applied based on their impact on observations. This means detail in the model is automatically kept where it is needed and discarded where it is not.

*This work was supported in part by the NSF under grant numbers EPCN-1710727 and NSF-1753357.

[1]Benjamin L. Francis and Mark K. Transtrum are with the Department of Physics and Astronomy, Brigham Young University, Provo, UT, USA bfrancis17@byu.edu mktranstrum@byu.edu

[2]Andrija T. Sarić is with the Faculty of Technical Sciences, University of Novi Sad, Novi Sad, Serbia asaric@uns.ac.rs

[3]Aleksandar M. Stanković is with the Dept. of Electrical and Computer Engineering, Tufts University, Medford, MA, USA astankov@ece.tufts.edu

Despite these advantages, MBAM is impractical for very large systems. Finding appropriate parameter limits requires computationally intensive calculations that reveal only one parameter limit at a time. This is very tedious for models with thousands of parameters. In such cases it is helpful to split the model up into pieces to which MBAM can be applied. In other cases one may wish to reduce only part of the model and retain the remainder as-is. These scenarios illustrate the need for a piecemeal reduction strategy for MBAM.

In this paper, we reframe the problem of structure-preserving model reduction for networked systems in the context of MBAM. We first show that, when cast in terms of manifold boundaries, the model reduction problem is equivalent to selecting an optimal element from a partially ordered set (poset). We then leverage the mathematical properties of posets to identify appropriate model components for reduction. Posets can be written as the product of prime factors, similar to integers. We argue that these prime factors are the natural submodels for structure-preserving model reduction. The outline of the paper is as follows. Background material on information geometry and posets is given in Sec. II. We discuss models of networks and the properties of their model reduction posets in Sec. III. This is followed by a demonstration of structure-preserving model reduction on an example network. We then discuss our results, and we give concluding remarks in Sec. IV.

II. Background

A. Information geometry and model reduction

Consider the following 2nd-order continuous-time linear state space model:

$$\begin{bmatrix}\dot{x}_1(t)\\ \dot{x}_2(t)\end{bmatrix} = \begin{bmatrix}-\lambda_1 & 0\\ 0 & -\lambda_2\end{bmatrix}\begin{bmatrix}x_1(t)\\ x_2(t)\end{bmatrix} + \begin{bmatrix}1\\ 1\end{bmatrix} u(t) \quad (1)$$

$$y(t) = \begin{bmatrix}1 & 1\end{bmatrix} x(t). \quad (2)$$

This system can be solved exactly for $y(t)$, yielding (for the case of zero input, $u(t) = 0$)

$$y(t) = e^{-\lambda_1 t} + e^{-\lambda_2 t}, \quad (3)$$

where we have assumed, for simplicity, that $x_1(0) = x_2(0) = 1$ (see Fig. 1, left). Fixing a set of time points $\{t_1, t_2, t_3\}$ yields a vector of predictions $\mathbf{y} = [y(t_1), y(t_2), y(t_3)]^\intercal$. As parameters λ_1 and λ_2 are varied, $\mathbf{y}$ sweeps out a two-dimensional manifold in $\mathbb{R}^3$, called the *model manifold* [28], [29] (see Fig. 1, center).

In general, a model with N parameters which makes M predictions leads to an N-dimensional manifold embedded in $\mathbb{R}^M$. Faces, edges, corners, etc. of this manifold correspond to limiting approximations of the model, such as singular perturbations. These approximations form a *partially ordered set* (poset; see Sec. II-B) of reduced models with decreasing levels of both computational and statistical complexity [30] (see Fig. 1, right). We call this poset the manifold boundary reduction poset. The Manifold Boundary Approximation Method (MBAM) selects the reduced model from this poset that introduces the least error for a given level of complexity, or conversely the smallest complexity for a chosen error bound.

B. Partially ordered sets

A partially ordered set (poset) is a set $\mathcal{P}$ paired with an ordering relation $\leq_{\mathcal{P}}$. A *discrete* poset is a poset whose elements are countable. Discrete posets may be visualized with a Hasse diagram (see Fig. 1, right). The Cartesian product of two posets $\mathcal{P}$ and $\mathcal{Q}$ is defined as

$$\mathcal{P} \times \mathcal{Q} \equiv \{(F, G) | F \in \mathcal{P}, G \in \mathcal{Q}\}, \quad (4)$$

where the ordering is given by

$$(F, G) \leq_{\mathcal{P}\times\mathcal{Q}} (F', G') \text{ iff } F \leq_{\mathcal{P}} F' \text{ and } G \leq_{\mathcal{Q}} G'. \quad (5)$$

A poset $\mathcal{P}$ is *factorable* if there exist nontrivial $\mathcal{Q}_1$ and $\mathcal{Q}_2$ such that $\mathcal{P} = \mathcal{Q}_1 \times \mathcal{Q}_2$; otherwise, $\mathcal{P}$ is *prime*. All posets have a unique prime factorization [31]. In this work we consider the poset of manifold boundary reduced models and its prime factorization. The prime factorization leads to a natural decomposition of the model for performing structure preserving model reduction.

III. Networks and model reduction posets

A. Power systems network model

Consider a network of current-carrying conductors connected at various junctions/nodes (Fig. 2). Each network edge has an associated resistance R_{ik}, taken as a model parameter.[2] Assume each network node has both a constant input current I_i^{in} and resistive load R_i^{out} connected to ground, and that voltages V_i and outgoing currents I_i^{out} can be measured at nodes. Such a network is an idealization of typical power systems networks, where edges represent transmission lines and nodes represent buses to which generators (sources) and loads (sinks) are attached.

Current conservation at each node gives

$$I_i^{\text{in}} - I_i^{\text{out}} = \sum_{k=1}^{N_{\text{node}}} I_{ik}, \quad (6)$$

where I_{ik} is the current flowing from node i to node k (so $I_{ki} = -I_{ik}$). The voltage difference across each branch is given by

$$V_i - V_k = I_{ik} R_{ik}. \quad (7)$$

Finally, the outgoing current I_i^{out} from each node can be found using

$$V_i = I_i^{\text{out}} R_i^{\text{out}}. \quad (8)$$

Given the input currents I_i^{in} and resistive loads R_i^{out}, these three sets of equations can be solved for the node voltages V_i, branch currents I_{ik} (not observed), and outgoing currents I_i^{out} as a function of the branch resistances R_{ik}.

There are two relevant parameter limits for R_{ik} that arise from model reduction with MBAM, both of which

[2] We consider the DC case for simplicity. Analogous results hold for AC networks, where the magnitude of the admittance $|Y_{ik}|$, considered as a model parameter, plays the inverse role of the resistance R_{ik} (see [24], [25]).

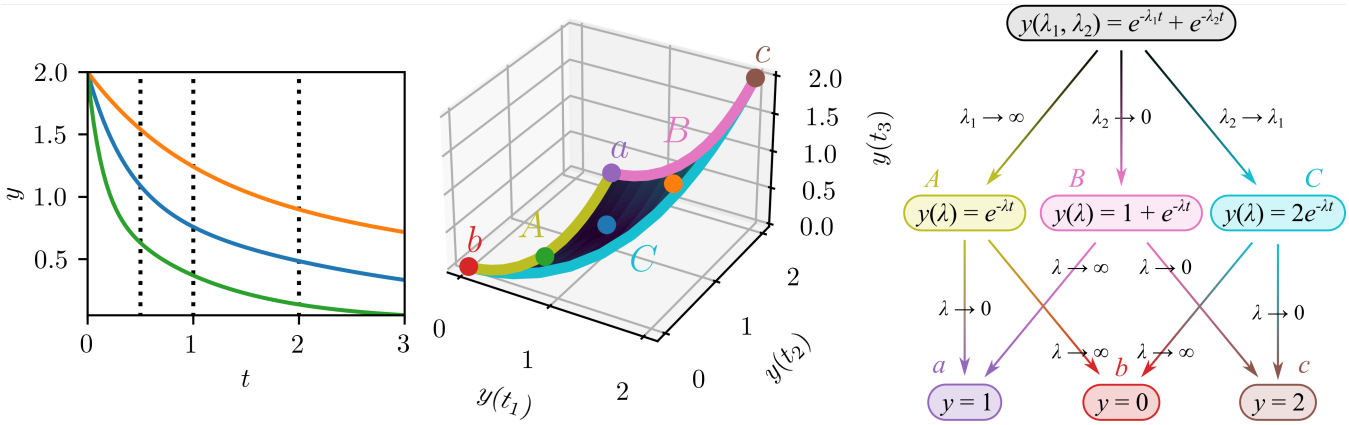

Fig. 1. Left: Time series predictions for the exponential model in Eq. (3) for three choices of λ_1 and λ_2. Center: Model manifold for the exponential model. Axes correspond to the three time "slices" (dotted lines) in the time series plot, and the three unlabeled points in the middle of the manifold correspond to the three time series curves whose colors they match. Right: Hasse diagram illustrating the poset of reduced models for the exponential model, corresponding to the boundary structure of the model manifold. Each level of the diagram has models with both fewer parameters and less computational complexity. The model is invariant to switching λ_1 and λ_2, so we have assumed $\lambda_1 > \lambda_2$ without loss of generality.

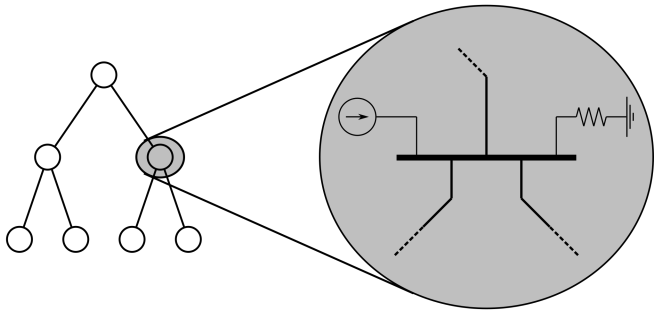

Fig. 2. Diagram for a network of current-carrying conductors. Each edge has an associated resistance. All nodes have both a current source and a resistive load (detail at right). Voltage and outgoing currents are measured at nodes.

are physically interpretable. Applying $R_{ik} \to 0$ in Eq. (7) simply gives $V_i = V_k$, i.e., the edge between nodes i and k contracts and the two nodes merge. On the other hand, $R_{ik} \to \infty$ gives $I_{ik} = 0$, i.e., the edge between nodes i and k is removed, disconnecting the nodes. Usually this is acceptable, with one exception. Letting $I_{ik} = 0$ for all k Eq. (6) leads to $I_i^{\text{out}} = I_i^{\text{in}}$, so if these are not equal then the last branch connecting node i to another node cannot be disconnected or its voltage will not remain finite. In the examples in this paper, we assume that all nodes have both a current source and a resistive load so that letting $R_{ik} \to \infty$ is always a valid limit. This means that both of the limits for R_{ik} result in reductions that respect conservation of current (charge) and power (energy), which guarantees the stability of the reduced models.

B. Network reduction posets

In the following, we denote an acyclic network with n edges as A_n and a network with n edges connected in a single simple cycle as C_n.

In the previous section, we showed that, when reducing a weighted network with MBAM, each edge can either be kept or be reduced in one of two ways. Accordingly, there are three model reduction "states" possible for each edge of the network: unreduced, removed, or contracted. We will denote these three states as u, r, and c, respectively. We denote the model reduction state X of a weighted network with n edges as the collection $X = (x_1, x_2, \ldots, x_n)$ of the states $x_i \in \{u, r, c\}$ of its edges. If we express the ordering on these edge states as $r \leq u$ and $c \leq u$, then this ordering can be extended to a state X of a network as follows: $X \leq X'$ iff $x_i \leq x_i' \ \forall i$.

A one-edge network A_1 has three possible reduction states, which are the three possible states of its edge: u, r, or c (Fig. 3a). The manifold boundary reduction poset of A_1 consists of these three states, with the aforementioned orderings (Fig. 3b). We denote this poset $\mathcal{P}(A_1)$.

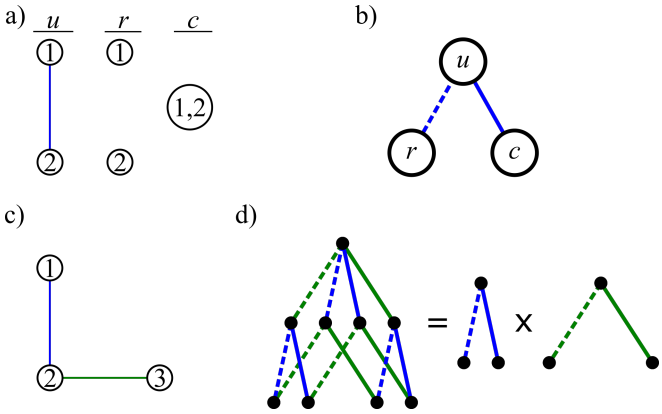

Fig. 3. (a) Reductions states of a one-edge network A_1: unreduced u, removed r, or contracted c. (b) Hasse diagram of the poset $\mathcal{P}(A_1)$ of reduction states of A_1, illustrating the orderings $r \leq u$ and $c \leq u$. A dashed line indicates edge removal and a solid line indicates edge contraction. (c) A two-edge network A_2. (d) Hasse diagram of the poset $\mathcal{P}(A_2)$ of reduction states of A_2, illustrating the factorization $\mathcal{P}(A_2) = \mathcal{P}(A_1) \times \mathcal{P}(A_1)$. The repeated appearance of these poset factors throughout the Hasse diagram is characteristic of a factorable poset.

Adding another node and branch changes A_1 into A_2 (Fig. 3c). In this case, reduction (contraction or removal) of one edge has no effect on the reduction of the other edge, so every state x_1 of the original edge may be paired with any state x_2 of the new edge and identified with a unique reduction state of A_2, i.e., element of $\mathcal{P}(A_2)$. That is, $\mathcal{P}(A_2) = \{X = (x_1, x_2) \,|\, x_1 \in \mathcal{P}(A_1),\, x_2 \in \mathcal{P}(A_1)\}$. The ordering in $\mathcal{P}(A_2)$ is such that $X \leq_{\mathcal{P}(A_2)} X'$ iff $x_1 \leq_{\mathcal{P}(A_1)} x_1'$ and $x_2 \leq_{\mathcal{P}(A_1)} x_2'$. Thus, $\mathcal{P}(A_2)$ conforms to the definition [Eqs. (4) and (5)] of the Cartesian product of two copies of $\mathcal{P}(A_1)$:

$$\mathcal{P}(A_2) = \mathcal{P}(A_1) \times \mathcal{P}(A_1) \equiv \mathcal{P}(A_1)^2 \tag{9}$$

(see Fig. 3d).

This generalizes to A_n; in fact, we have the following theorem:

Theorem 1. *The poset $\mathcal{P}(A_n)$ of manifold boundary reduced models of a weighted acyclic network A_n with n edges is the Cartesian product of n copies of the poset $\mathcal{P}(A_1)$ for a weighted one-edge network A_1:*

$$\mathcal{P}(A_n) = \mathcal{P}(A_1)^n. \tag{10}$$

Proof. We give a proof by induction. The case $n = 1$ is trivial. Next, assume Eq. (10) is true for some $n \geq 1$. As long as no cycles are created, adding an edge (and an appropriate node) to an n-edge acyclic network A_n creates an $(n+1)$-edge acyclic network A_{n+1}. Reduction of the original network A_n has no effect on reduction of the newly added edge, so every state X of A_n may be paired with any state x_{n+1} of the new edge and identified with a unique reduction state of A_{n+1}, i.e., element of $\mathcal{P}(A_{N+1})$. Thus, we can write $\mathcal{P}(A_{N+1}) = \{Y = (X, x_{n+1}) \,|\, X \in \mathcal{P}(A_n),\, x_{n+1} \in \mathcal{P}(A_1)\}$. $Y \leq_{\mathcal{P}(A_{N+1})} Y'$ implies that $x_i \leq x_i'$ for each individual edge, which implies both $X \leq_{\mathcal{P}(A_n)} X'$ and $x_{n+1} \leq_{\mathcal{P}(A_1)} x_{n+1}'$. Likewise, $X \leq_{\mathcal{P}(A_n)} X'$ and $x_{n+1} \leq_{\mathcal{P}(A_1)} x_{n+1}'$ together imply that $x_i \leq x_i'$ for each edge, and hence that $Y \leq_{\mathcal{P}(A_{N+1})} Y'$. Thus, by Eqs. (4) and (5),

$$\mathcal{P}(A_{n+1}) = \mathcal{P}(A_n) \times \mathcal{P}(A_1). \tag{11}$$

Finally, since we have assumed Eq. (10) is true for n, we can write

$$\mathcal{P}(A_{n+1}) = \mathcal{P}(A_1)^n \times \mathcal{P}(A_1) = \mathcal{P}(A_1)^{n+1}. \tag{12}$$

Thus, if Eq. (10) is true for n, it is also true for $n+1$. □

This means that an acyclic network can be divided into arbitrary pieces and each reduced by MBAM individually, because every reduction state of each edge is compatible with every other.

The proof of Theorem 1 relied on the acyclic property of the network. We now show that the network reduction poset for a cycle is always prime. First a lemma:

Lemma 1. *The poset $\mathcal{P}(C_3)$ of manifold boundary reduced models of a weighted 3-cycle network C_3 is prime.*

Proof. We give a proof by contradiction. First, assume $\mathcal{P}(C_3)$ is factorable. Then it can be written as a product $\mathcal{P}(C_3) = \mathcal{Q}_1 \times \mathcal{Q}_2$. The only nontrivial candidates for the factors $\mathcal{Q}_i$ are the posets $\mathcal{P}(A_1)$ and $\mathcal{P}(A_2)$ for the acyclic networks A_1 and A_2. Factorability of $\mathcal{P}(C_3)$ then dictates that there exist an element of $\mathcal{P}(C_3)$ (state of C_3) corresponding to every pair of elements from $\mathcal{P}(A_1)$ and $\mathcal{P}(A_2)$ (states of A_1 and A_2). Consider the states c of A_1 and (u, u) of A_2. There is no state of C_3 that is compatible with both of these states because contracting an edge results in a network where only one edge is identifiable, equivalent to both the (r, u) and (u, r) states of A_2 but not to (u, u) (see Fig. 4). There are no other candidates with which to factorize $\mathcal{P}(C_3)$, so it is prime. □

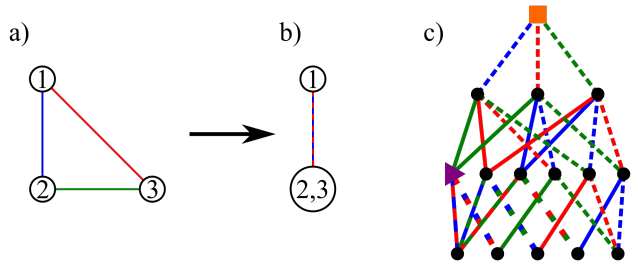

Fig. 4. (a) The cyclic network C_3. (b) Contracting the edge between nodes 2 and 3 leads to a one-edge network, because the blue and red edges are no longer individually identifiable from observations made at the nodes. (c) Hasse diagram for the model reduction poset of the 3-cycle network in (a). Some edges are multicolored because it is ambiguous which network edge remains at that point in the reduction. The networks in (a) and (b) are marked by the colored square and triangle, respectively.

We now show that the reduction posets of n-cycle networks are also prime for arbitrary n.

Theorem 2. *The poset $\mathcal{P}(C_n)$ of manifold boundary reduced models of a weighted n-cycle network C_n is prime.*

Proof. As in Lemma 1, we only need to find a single pair of incompatible states for each candidate pair of poset factors to show that $\mathcal{P}(C_n)$ is prime. The candidates are the posets $\mathcal{P}(A_k)$ and $\mathcal{P}(A_{n-k})$, where $1 \leq k \leq n/2$. By contracting enough edges, it is always possible to reduce C_n to C_3, A_k to A_1, and A_{n-k} to A_2. This reproduces the situation in Lemma 1, that is to say, the state $(c, \ldots, c)$ of A_k is incompatible with the state $(c, \ldots, c, u, u)$ of A_{n-k} (and other similar states with two u edges and the rest c). Therefore $\mathcal{P}(C_n)$ is prime. □

C. Acyclic network example

In Sec. III-B, we showed that an acyclic network can be divided arbitrarily and reduced piece by piece using MBAM. Here we demonstrate this using the acyclic network shown in Fig. 5a. As discussed in Sec. III-A, we simulated the flow of current through the network by assigning a random value for each branch resistance and calculating node voltages and outgoing currents for a variety of choices of input currents. We then divided the network into the five subnetworks shown and reduced them individually using MBAM. The resulting

reduced network, shown in Fig. 5b, represents a simplified effective network whose behavior closely approximates that of the original. In some cases, branch resistances are large enough that almost no current flows, which is approximately equivalent to having no branch in those places. In others, branch resistances are small enough that the voltages on the adjoining nodes are nearly equal, and can be approximated as if they are equal.

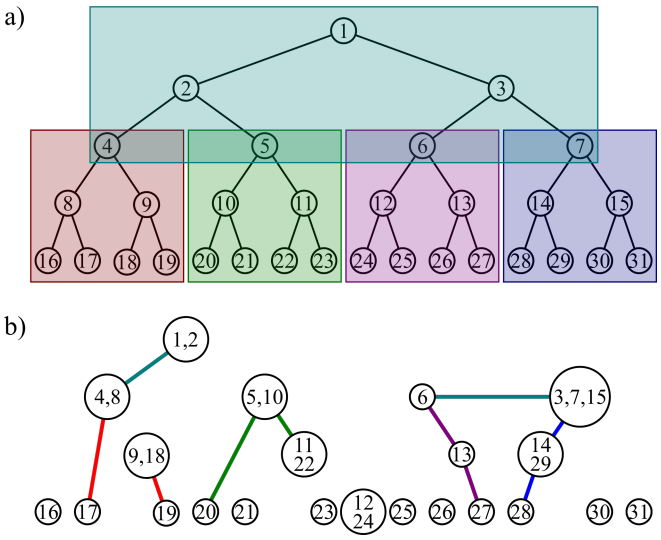

Fig. 5. (a) An example acyclic network. Each shaded box is a subnetwork to be reduced separately. (b) The final reduced network, with some branches removed and some nodes merged, representing the effective interactions between nodes.

As the reduction with MBAM proceeds, error is introduced into the model in the form of bias. An acceptable level of bias will depend on the application—for example, informed by the noise in the available measurements. For this study, we arbitrarily ended the reduction when 2/3 of the parameters had been eliminated, but in principle, the method allows the user to achieve any desired level of tradeoff between bias and complexity.

Recall that MBAM selects a reduced model from a poset of possible reduced models. To evaluate how well the MBAM-selected model approximates the unreduced model, we calculated the model bias,

$$\text{bias}^2 = \sum_i (y_i - \tilde{y}_i)^2, \tag{13}$$

which compares the predictions y_i of the original model and $\tilde{y}_i$ of the reduced model. We compared this with the model bias for 1000 other reduced models that could have been selected in Fig. 6. In each of these other reduced models, we randomly selected 2/3 of the parameters (branch resistances) and set them either to 0 or ∞ so that they have the same complexity as the MBAM-selected model. The MBAM-selected model introduces less bias than any of the others.

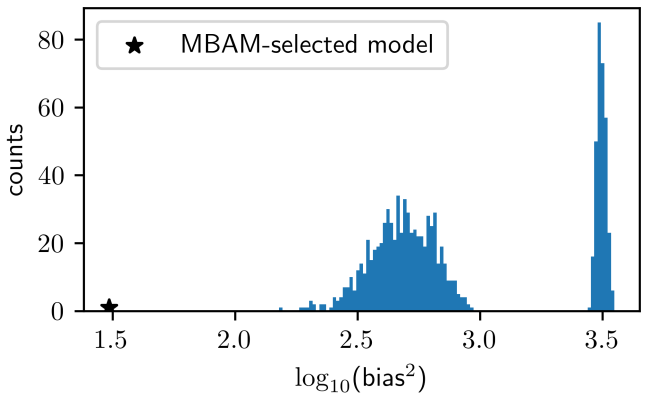

Fig. 6. Histogram of model biases for 1000 possible reduced models with 2/3 of the parameters randomly set either to 0 or ∞.

D. Discussion

Determining the prime factors in the network reduction poset is important because of its implications for dividing a network into subnetworks for doing piecemeal model reduction. Theorem 1 shows that network edges that are not part of cycles can be split up or grouped arbitrarily. The same is not true for edges that are part of cycles because it is possible for the reduced states of the subnetworks to be incompatible with each other. Consider the partial network shown in Fig. 7. Contracting any of the edges along the boundary could lead to the situation in Fig. 4b where two edges become individually unidentifiable. A similar situation can occur for a larger cycle split by a subnetwork boundary, because contracting enough edges of a cycle eventually leads to a 3-cycle.

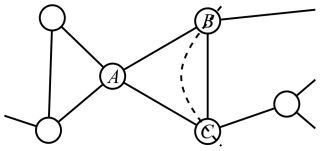

Fig. 7. Part of a network showing a subnetwork boundary (dashed line) that intersects a 3-cycle. Separately reducing the left and right subnetworks could lead to the situation in Fig. 4b where two edges become individually unidentifiable. On the left, this would occur if either of edges AB or AC were contracted. On the right, it would happen if edge BC was contracted.

This seems to indicate that parts of a network containing cycles can never be broken up and reduced piecewise, which is problematic considering that many power systems networks involve interconnected cycles. However, when a network is large enough, the upper levels of the associated Hasse diagram are identical to the Hasse diagram of a factorable poset (see Fig. 8) and can be treated as if they were factorable. Specifically, it is only along subnetwork boundaries (Fig. 7) that situations like the one in Fig. 4b may arise. To avoid these situations, no edge connected to a node on a subnetwork boundary should be contracted.

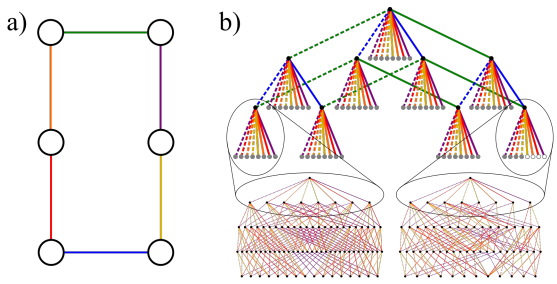

Fig. 8. (a) The 6-cycle network C_6 and (b) part of the Hasse diagram for its reduction poset. Edges and nodes descending from gray and white nodes in the Hasse diagram have been omitted for clarity, with the exception of the subsets shown below. At gray nodes, each remaining edge in the network may still be either removed or contracted. At white nodes, the network has been reduced to a 3-cycle, so only the option to remove an edge is available. Although the repeating structure of the diagram does not carry through to the lower levels (notice the differences in the subsets at the bottom), the first few levels have the same structure as that of the factorable poset in Fig. 3b.

IV. Conclusions

In this paper, we have shown how to split a network into subnetworks that can reduced individually using the Manifold Boundary Approximation Method (MBAM). This decomposition of the network is based on the prime factorization of a partially ordered set of reduced models of the undivided network. We have demonstrated structure-preserving model reduction on an acyclic network. The resulting network topology reflects the salient features of the network while eliminating unnecessary detail.

This work has established the foundation for piecemeal model reduction of networks via MBAM. Real networks often have both acyclic subnetworks as well as cycles. The method presented here can be applied to the acyclic subnetworks of any network. Future work will address networks with cycles.

References

[1] H. Yu, L. He, and S. Tar, "Block structure preserving model order reduction," in *BMAS 2005. Proceedings of the 2005 IEEE International Behavioral Modeling and Simulation Workshop, 2005.* IEEE, 2005, pp. 1–6.

[2] L. Li and F. Paganini, "Structured coprime factor model reduction based on lmis," *Automatica*, vol. 41, no. 1, pp. 145–151, 2005.

[3] A. Vandendorpe and P. Van Dooren, "Model reduction of interconnected systems," in *Model order reduction: theory, research aspects and applications*. Springer, 2008, pp. 305–321.

[4] H. Sandberg and R. M. Murray, "Model reduction of interconnected linear systems," *Optimal Control Applications and Methods*, vol. 30, no. 3, pp. 225–245, 2009.

[5] H. Sandberg, "An extension to balanced truncation with application to structured model reduction," *IEEE Transactions on Automatic Control*, vol. 55, no. 4, pp. 1038–1043, 2010.

[6] C. Sturk, L. Vanfretti, Y. Chompoobutrgool, and H. Sandberg, "Coherency-independent structured model reduction of power systems," *IEEE Transactions on Power Systems*, vol. 29, no. 5, pp. 2418–2426, 2014.

[7] X. Cheng, Y. Kawano, and J. M. Scherpen, "Model reduction of multi-agent systems using dissimilarity-based clustering," *IEEE Transactions on Automatic Control*, vol. 64, no. 4, pp. 1663–1670, 2018.

[8] R. A. Date and J. H. Chow, "Aggregation properties of linearized two-time-scale power networks," *IEEE Transactions on Circuits and Systems*, vol. 38, no. 7, pp. 720–730, 1991.

[9] E. Bıyık and M. Arcak, "Area aggregation and time-scale modeling for sparse nonlinear networks," *Systems & Control Letters*, vol. 57, no. 2, pp. 142–149, 2008.

[10] D. Romeres, F. Dörfler, and F. Bullo, "Novel results on slow coherency in consensus and power networks," in *2013 European Control Conference (ECC)*. IEEE, 2013, pp. 742–747.

[11] M. L. Ourari, L.-A. Dessaint, and V.-Q. Do, "Dynamic equivalent modeling of large power systems using structure preservation technique," *IEEE Transactions on Power Systems*, vol. 21, no. 3, pp. 1284–1295, 2006.

[12] U. Annakkage, N.-K. C. Nair, Y. Liang, A. Gole, V. Dinavahi, B. Gustavsen, T. Noda, H. Ghasemi, A. Monti, M. Matar *et al.*, "Dynamic system equivalents: A survey of available techniques," *IEEE Transactions on Power Delivery*, vol. 27, no. 1, pp. 411–420, 2011.

[13] X. Lei, D. Povh, and O. Ruhle, "Industrial approaches for dynamic equivalents of large power systems," in *2002 IEEE Power Engineering Society Winter Meeting. Conference Proceedings (Cat. No. 02CH37309)*, vol. 2. IEEE, 2002, pp. 1036–1042.

[14] S. M. Ashraf, B. Rathore, and S. Chakrabarti, "Performance analysis of static network reduction methods commonly used in power systems," in *2014 Eighteenth National Power Systems Conference (NPSC)*. IEEE, 2014, pp. 1–6.

[15] C. Grudzien, D. Deka, M. Chertkov, and S. N. Backhaus, "Structure- and physics-preserving reductions of power grid models," *Multiscale Modeling & Simulation*, vol. 16, no. 4, pp. 1916–1947, 2018.

[16] M. K. Transtrum and P. Qiu, "Model reduction by manifold boundaries," *Physical review letters*, vol. 113, no. 9, p. 098701, 2014.

[17] ——, "Bridging mechanistic and phenomenological models of complex biological systems," *PLoS computational biology*, vol. 12, no. 5, 2016.

[18] G. Bohner and G. Venkataraman, "Identifiability, reducibility, and adaptability in allosteric macromolecules," *Journal of General Physiology*, vol. 149, no. 5, pp. 547–560, 2017.

[19] D. M. Lombardo and W.-J. Rappel, "Systematic reduction of a detailed atrial myocyte model," *Chaos: An Interdisciplinary Journal of Nonlinear Science*, vol. 27, no. 9, p. 093914, 2017.

[20] M. K. Transtrum, A. T. Sarić, and A. M. Stanković, "Measurement-directed reduction of dynamic models in power systems," *IEEE Transactions on Power Systems*, vol. 32, no. 3, pp. 2243–2253, 2016.

[21] ——, "Information geometry approach to verification of dynamic models in power systems," *IEEE Transactions on Power Systems*, vol. 33, no. 1, pp. 440–450, 2017.

[22] A. T. Sarić, M. K. Transtrum, and A. M. Stanković, "Information geometry for model identification and parameter estimation in renewable energy–dfig plant case," *IET Generation, Transmission & Distribution*, vol. 12, no. 6, pp. 1294–1302, 2017.

[23] C. C. Youn, A. T. Sarić, M. K. Transtrum, and A. M. Stanković, "Information geometry for model reduction of dynamic loads in power systems," in *2017 IEEE Manchester PowerTech*. IEEE, 2017, pp. 1–6.

[24] M. K. Transtrum, B. L. Francis, A. T. Sarić, and A. M. Stanković, "Simultaneous global identification of dynamic and network parameters in transient stability studies," in *2018 IEEE Power & Energy Society General Meeting (PESGM)*. IEEE, 2018, pp. 1–5.

[25] B. L. Francis, J. R. Nuttall, M. K. Transtrum, A. T. Sarić, and A. M. Stanković, "Network reduction in transient stability models using partial response matching," in *2019 North American Power Symposium (NAPS)*. IEEE, 2019, pp. 1–6.

[26] T. Nikšić and D. Vretenar, ""sloppy" nuclear energy density functionals: Effective model reduction," *Physical Review C*, vol. 94, no. 2, p. 024333, 2016.

[27] P. E. Paré, D. Grimsman, A. T. Wilson, M. K. Transtrum, and S. Warnick, "Model boundary approximation method as a unifying framework for balanced truncation and singular perturbation approximation," *IEEE Transactions on Automatic Control*, vol. 64, no. 11, pp. 4796–4802, 2019.

[28] M. K. Transtrum, B. B. Machta, and J. P. Sethna, "Why are nonlinear fits to data so challenging?" *Physical review letters*, vol. 104, no. 6, p. 060201, 2010.

[29] ——, "Geometry of nonlinear least squares with applications to sloppy models and optimization," *Physical Review E*, vol. 83, no. 3, p. 036701, 2011.

[30] M. K. Transtrum, G. Hart, and P. Qiu, "Information topology identifies emergent model classes," *arXiv preprint arXiv:1409.6203*, 2014.

[31] I. Gleason and I. Hubard, "Products of abstract polytopes," *Journal of Combinatorial Theory, Series A*, vol. 157, pp. 287–320, 2018.